

# THERMAL INERTIA OF HOLLOW WALL BLOCKS: ACTUAL BEHAVIOR AND MYTHS

M. Cianfrini<sup>1</sup>; M. Corcione<sup>2</sup>; R. de Lieto Vollaro<sup>1</sup>; E. Habib<sup>2</sup>; A. Quintino<sup>2</sup>

1: DIMI – Università degli Studi Roma Tre, via della Vasca Navale, 79 - 00146, Rome, Italy

2: DIAEE – Sapienza Università di Roma, via Eudossiana, 18 - 00184, Rome, Italy

## ABSTRACT

In the context of growing requirements to save energy in buildings and high objectives for Net Zero Energy Buildings (NZEBs) in Europe, strong emphasis is placed on the thermal performance of building envelopes, and in particular on thermal inertia to save cooling energy.

High thermal inertia of outer walls leads to a mitigation of the daily heat wave, reducing cooling peak load and energy demand. Moreover, building envelopes with high heat capacity act as heat storages, increasing the effectiveness of natural ventilation for thermal comfort through a night-day energy shifting.

Even though there are some papers available in the open literature on dynamic heat transfer through hollow bricks, yet common calculation methods are applicable to homogeneous layers only. That is the case of ISO 13786 regulation "Thermal performance of building components - Dynamic thermal characteristics - Calculation methods", for example. On the other hand, hollow blocks are very commonly used in building envelopes. Thus, available methods are not suitable for prediction of dynamic thermal performances.

On the other hand, the widely common assumption that high mass means high thermal inertia leads to the use of higher mass blocks or bricks. Yet, numerical and experimental studies on thermal inertia of hollow envelope-components have not confirmed this general assumption, even though no systematic analysis has been found in the open literature.

In this framework, numerical simulations of the thermal performance of hollow bricks have been done with a specifically-developed finite-difference computational code. Three common basic shapes with different void fraction and thermal properties have been analyzed with a triangular pulse solicitation, in order to highlight the relevance of front mass and other parameters on the thermal inertia, measured through heat wave delay.

Results show that wall front mass is often misleading as thickness, number of cavities and clay thermal diffusivity are more important.

*Keywords: building envelope, thermal inertia, hollow block, thermal pulse response*

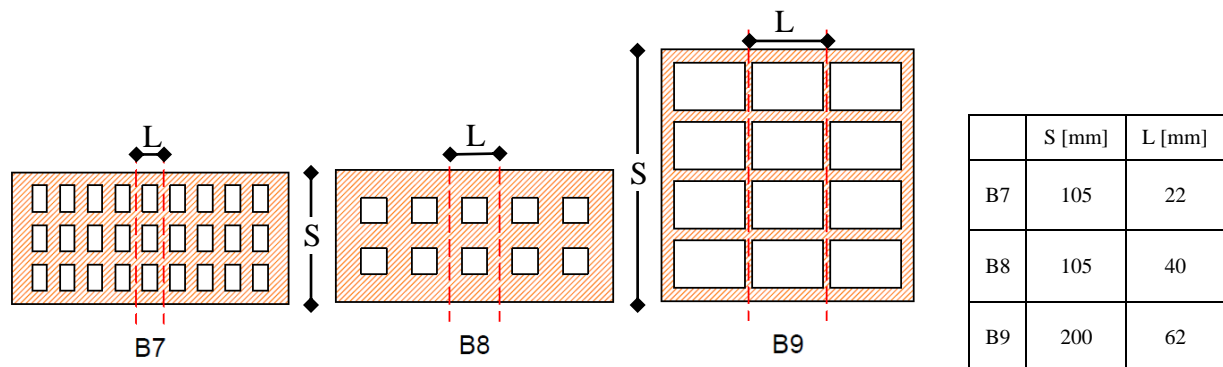


Figure 1: Sketch of the masonry units and integration domains.

## INTRODUCTION

Dynamic heat transfer through building envelopes has been extensively studied, being of fundamental importance in building energy analysis. Different methods for the calculation of the heat gain through exterior roofs and walls are reported in [1] and [2]. However, as these methods apply uniquely to roofs and walls consisting of homogeneous layers, their employment is not suitable for common building envelopes. A limited number of studies are readily available in the open literature on the dynamic thermal features of non-homogeneous building components.

Lacarrière et al. [3] and Sala et al. [4] performed experimental studies with step and triangular pulse solicitation on hollow blocks arriving to different results. The first has found out that the effective specific heat per unit volume of the block was of the same order of that of the solid part of the masonry unit. The latter has found that the effective specific heat per unit volume resulted to be nearly one half of that of the clay which the solid part of the block consisted of. Regarding the numerical approach to the problem, some studies are available [5-7], with very different methods and envelope elements, thus their results are hardly comparable.

In this framework, the aim of the present study is to point out whether front mass is actually straight connected to thermal inertia. A two dimensional numerical study is performed under the assumption that the investigated brick is subjected to a triangular temperature pulse on one side. B7, B8 and B9 blocks among those reported in EN1745 [8] are chosen as much simplification of integration domain is possible. Reference masonry material is clay of three different densities as shown in Table 1.

	$c_p$ (J/kg K)	$\rho$ (kg/m <sup>3</sup> )	$c_p \cdot \rho$ (kJ/m <sup>3</sup> K)	$k$ (W/m K)	$\alpha$ (m <sup>2</sup> /s)
LWC – Light Weight Clay	1000	1000	1000	0,27	0,27 x 10 <sup>-6</sup>
MWC – Medium Weight Clay	1000	1700	1700	0,51	0,30 x 10 <sup>-6</sup>
HWC – Heavy Weight Clay	1000	2400	2400	0,84	0,35 x 10 <sup>-6</sup>

Table 1: Properties of masonry material [8].

## MATHEMATICAL FORMULATION AND COMPUTATIONAL PROCEDURE

The reference masonry units are sketched in fig. 1. Real walls have mortar all around the block, giving fully 3-dimensional thermal field. As this study is meant to be a first approach to the phenomenon, a simpler field is studied, neglecting both the effect of mortar, of the lateral edges and of plaster or any other layer in the wall. The computational domains are the parts limited by dashed lines, including a line of cavities.

Thermal field equation is described by a Cartesian two-dimensional Fourier's equation for conducting fields.

In cavities, convection contribution to heat transfer is neglected as Rayleigh numbers are very low, even in vertical arrangement. So, radiation heat transfer is superimposed to conduction. At cavity boundary, heat flux conservation is given by:

$$k_a \left. \frac{\partial T}{\partial n} \right|_a + q_R = k_c \left. \frac{\partial T}{\partial n} \right|_c \quad (1)$$

where,  $k$  stands for thermal conductivity,  $T$  for temperature,  $n$  for direction perpendicular to boundary, either  $x$  or  $y$ ,  $q_R$  for radiation heat transfer toward the cavity, and subscript  $a$  is for air and  $c$  is for clay. Radiation heat transfer is calculated through radiosity method with Hottel's crossed-string method for view factors.

Triangular pulse excitation is used to check dynamic heat transfer characteristics as it allows to simply identify heat transfer response in terms of time-lag, delay between pulse and response peak, and a damping degree, that is the ratio of stationary heat transfer at maximum temperature difference to actual peak heat transfer (equivalent to the reciprocal of decrement factor defined in [2]). A 1 K high, 2 hours wide pulse was chosen, with 20°C initial temperature. Along domain boundaries defined by the dashed lines, adiabatic condition is assumed, while the outer face that is not subject to the pulse is kept at constant temperature.

The governing equation, along with boundary and initial conditions stated above is solved through a control-volume formulation of the finite-difference method. A first-order backward scheme is used for time stepping. Radiation heat transfer is solved using the same faces of control volumes. The discretized equations lead to a linear system for conduction and for radiation in each cavity (as unknowns are radiation heat transfer). Iterative Jacobi algorithm [9] has been implemented to solve each system. At each time step, the conduction field is solved with previous radiation heat transfer that is then calculated in relation to the newly calculated cavity boundary temperatures, iteratively, up to when the new calculated radiation heat transfer is close to the previous one.

The average heat flux through constant temperature face (of length L) is calculated as:

$$q = \frac{1}{L} \int_0^L k_c \frac{\partial T}{\partial y} dx \quad (2)$$

The code was checked against reference simple analytic solutions, details can be found in [10]. Moreover, a self consistence test was conducted to get the optimal mesh-size, time step and variance limit for iterations. A 5 s time step and  $10^{-4}$  variance limit has been found to be a good balance between calculation time and solution accuracy with mesh sizes between 21x103 and 44x210, depending on cavity number and geometry.

## RESULTS

Numerical simulations have been performed for each kind of block, with the different types of clay. Cavities size in each block has been varied: for B7 type, with void fraction from 0% (full block) to 60% (standard blocks are 33%); for B8 type, with void fraction from 0% (full block) to 50% (standard blocks are 19%); for B9 type, with void fraction from 0% (full block) to standard one that is 69%. Cavities number and sides length ratio has been kept constant as well.

For each configuration, ratio of maximum heat flux under triangular pulse to heat flux under constant temperature difference was calculated as well as the delay between pulse peak and heat flux peak, as shown in fig. 2. Time-lag and decrement factor results are plotted against void fraction and front mass in figs. 3 to 5 for each block and clay type.

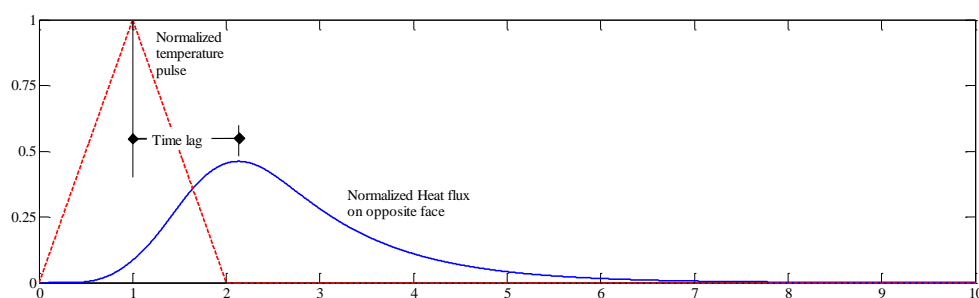


Figure 2: Temperature solicitation and heat flux response for B7 MWC block

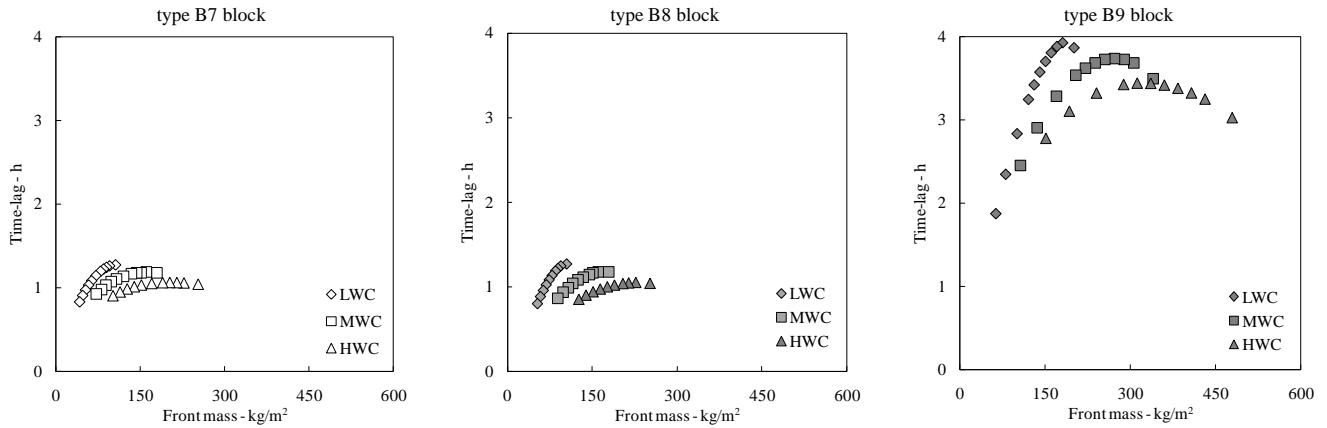


Figure 3: Time-lag vs. front mass

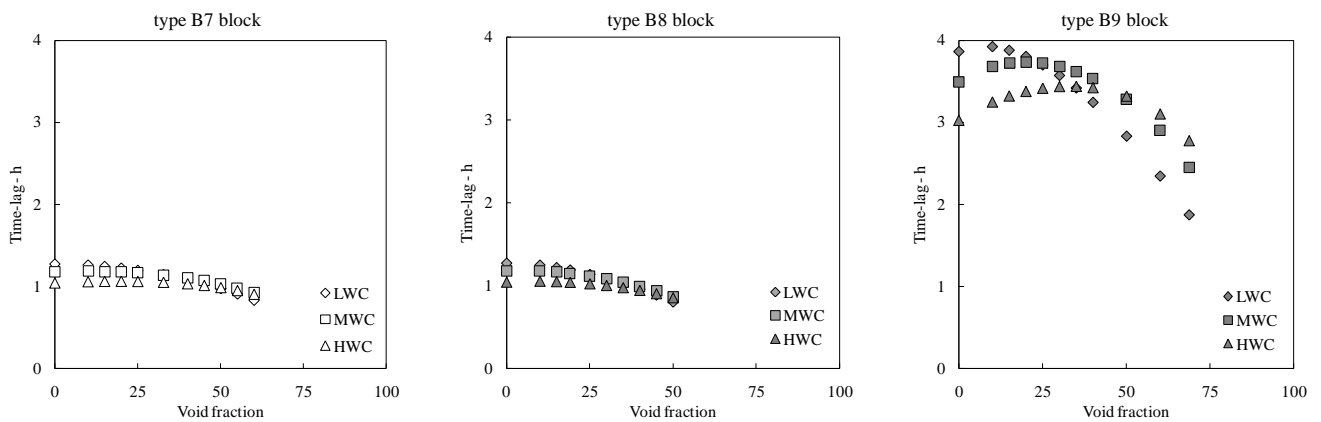


Figure 4: Time-lag vs. void fraction

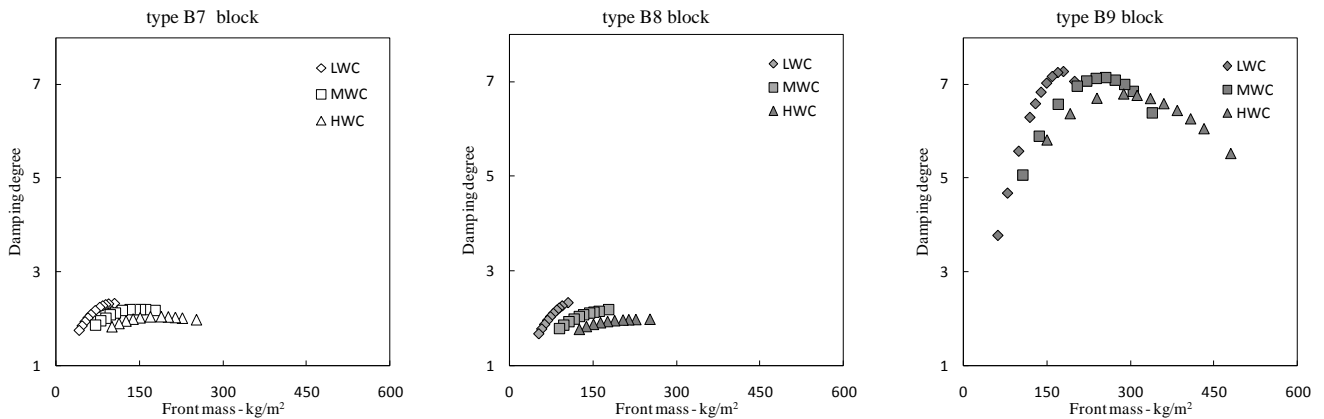


Figure 5: Damping degree vs. front mass

## DISCUSSION

Results show that time-lag is far from being simply connected to front mass. Once the block type is given, lighter clays will give higher time-lags. Actually, lighter clays have lower thermal diffusivity and thus are less reactive to thermal solicitation. This is clearly shown by looking at time lag values of full blocks (the right-end of each sequence). Comparing these to thermal diffusivity and block thickness a direct proportion is found to the square of thickness divided by thermal diffusivity, as shown in fig. 6.

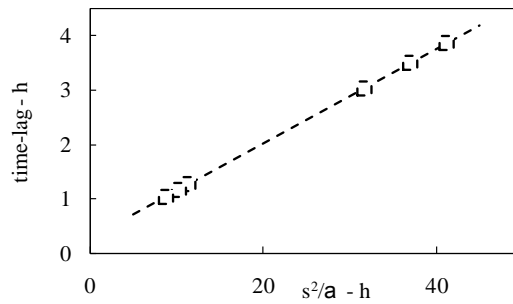


Figure 6: Full blocks, relation between time lag, thickness and thermal diffusivity

Moreover, at a given thickness and diffusivity of clay, higher front mass (due to smaller cavities) is linked to higher decrement factors only as long as void fraction is high. At low void fraction, time lag is insensitive to front mass for B7 and B8 block types. For B9 block type, at low void fractions, sensitivity of time lag to front mass is inverted, being lower for higher masses, especially for high thermal diffusivity clay. This could be due to a different effect of these small cavities: heat flux is not much reduced by cavities but, since it has to "go around" the cavities, the actual propagation length is increased, leading to a higher time-lag. This is more prominent in high diffusivity materials, in which the contribution to heat transfer of the instantaneous heat transfer by radiation across the cavity is less effective.

For light weight clay blocks, for each type, a straight dependence of time-lag to front mass is apparent, even though very different values are found for different blocks. The block types diverge for thickness and number of cavities. By normalizing time-lag with respect to these values, that is dividing time lag by block thickness and number of cavities, all the results appear to be quite aligned, as shown in fig. 7. This is not found for heavier clay blocks.

Moreover, comparing time-lag and damping degree, a linear correlation exists, as shown in fig. 8 and stated by eq. (3) with a standard deviation of 3.6%:

$$d = 1.9 \cdot \Delta\tau \quad (3)$$

where  $d$  is damping degree and  $\Delta\tau$  is time lag (in hours).

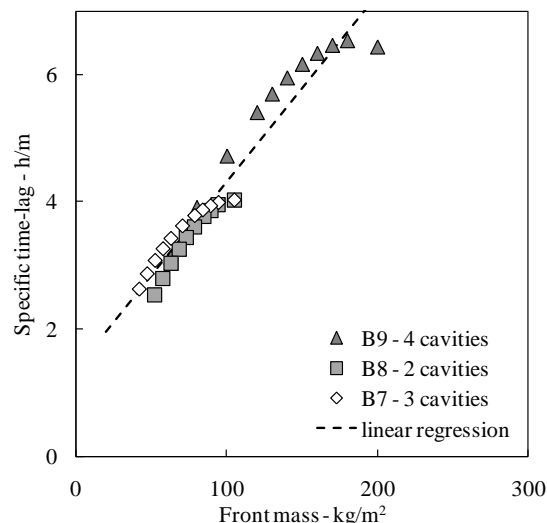


Figure 7: Specific time lag vs. front mass for light weight clay blocks, all types

## CONCLUSION

Temperature pulse response of hollow blocks has been numerically studied for different block types, cavities size and clay. Even though there is some correlation between front mass and time-lag, cavities and block thickness play a major role. Thus, as a general rule, thicker blocks will give higher thermal inertia.

Nonetheless this is just a first approach to a wide field of research showing unexpected results. Much more work should be done in order to fully understand unsteady behaviour of hollow blocks. As there is a strict correlation between the newly defined damping degree and time-lag, analysis can be focused on the latter to figure out behaviour.

## REFERENCES

1. ASHRAE Handbook – Fundamentals, ASHRAE, 2005
2. EN ISO 13786:1999 Thermal performances of building components – Dynamic thermal characteristics – Calculation methods
3. B. Lacarrière, A. Trombe, F. Monochoux: Experimental unsteady characterization of heat transfer in a multi-layer wall including air layers – Application to vertically perforated bricks, *Energy and Buildings* 38 (2006) 232-237
4. J.M. Sala, A. Urresti, K. Mrtin, I. Flores, A. Apaolaza: Static and dynamic thermal characterisation of a hollow brick wall: Tests and numerical analysis, *Energy and Buildings* 40 (2008) 1513-1520
5. K.C.K. Vijaykumar, P.S.S. Srinivasan, S. Dhandapani: A performance of hollow clay tile (HCT) laid reinforced cement concrete (RCC) roof for tropical summer climate, *Energy and Buildings* 39 (2007) 886-892
6. Z.L. Zhang, B.J. Wachenfeldt: Numerical study on the heat storing capacity of concrete walls with air cavities, *Energy and Buildings* 41 (2009) 769-773
7. G.H. Dos Santos, N. Mendes: Heat, air and moisture transfer through hollow porous blocks, *Int. J. Heat Mass Trans.* 52 (2009) 2390-2398
8. EN 1745:2002 Masonry and masonry products – Methods for determining design thermal values
9. L. Gori: Calcolo numerico (*in Italian*), Edizioni Kappa, 1999
10. C. Cianfrini, M. Corcione, E. Habib: Dynamic Thermal Features of Insulated Concrete Bricks, Proc. of 7<sup>th</sup> HEFAT conference, pp. 1065-1071 Antalya, Turkey, 2010

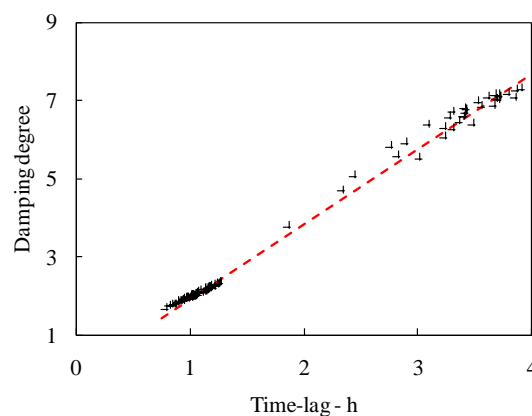


Figure 8: Damping degree vs. time-lag for all block types and void fractions